

 Open access • Posted Content • DOI:10.1101/2020.08.18.20177303

Role of IgM and IgA Antibodies in the Neutralization of SARS-CoV-2. — Source link

Jéromine Klingler, Weiss S, Weiss S, Xiaomei Liu ...+22 more authors

Institutions: Icahn School of Medicine at Mount Sinai, Veterans Health Administration, Mount Sinai Hospital, New York University

Published on: 24 Dec 2020 - The Journal of Infectious Diseases (Cold Spring Harbor Laboratory Press)

Topics: Neutralization and Antibody

Related papers:

- [IgA dominates the early neutralizing antibody response to SARS-CoV-2.](#)
- [Convergent antibody responses to SARS-CoV-2 in convalescent individuals.](#)
- [Enhanced SARS-CoV-2 neutralization by dimeric IgA.](#)
- [A serological assay to detect SARS-CoV-2 seroconversion in humans.](#)
- [Structure, Function, and Antigenicity of the SARS-CoV-2 Spike Glycoprotein.](#)

Share this paper:    

View more about this paper here: <https://typeset.io/papers/role-of-igm-and-iga-antibodies-in-the-neutralization-of-sars-197n84xuvv>

1
2
3
4
5
6
7
8
9
10
11
12
13
14
15
16
17
18
19
20
21
22
23
24
25

Role of IgM and IgA Antibodies in the Neutralization of SARS-CoV-2

Running title: Neutralization of SARS-CoV-2 by IgM and IgA

Jéromine Klingler^{1,2}, Svenja Weiss^{1,2}, Vincenza Itri¹, Xiaomei Liu^{1,2}, Kasopefoluwa Y. Oguntuyo³,
Christian Stevens³, Satoshi Ikegame³, Chuan-Tien Hung³, Gospel Enyindah-Asonye¹, Fatima Amanat^{3,4},
Ian Baine⁵, Suzanne Arinsburg⁵, Juan C. Bandres², Erna Milunka Kojic⁶, Jonathan Stoever⁷, Denise
Jurczynszak^{3,4}, Maria Bermudez-Gonzalez³, Arthur Nádás⁸, Sean Liu^{1,3}, Benhur Lee³, Susan Zolla-
Pazner^{1,3*}, Catarina E. Hioe^{1,2,3*}

¹Division of Infectious Diseases, Department of Medicine, Icahn School of Medicine at Mount Sinai, New York, NY USA.

²James J. Peters VA Medical Center, Bronx, NY, USA.

³Department of Microbiology, Icahn School of Medicine at Mount Sinai, New York, NY, USA.

⁴Graduate School of Biomedical Sciences, Icahn School of Medicine at Mount Sinai, New York, NY, USA.

⁵Department of Pathology, Icahn School of Medicine at Mount Sinai, New York, NY, USA.

⁶Division of Infectious Diseases, Department of Medicine, Mount Sinai West and Morningside, NY, USA.

⁷Pulmonary and Critical Care Medicine, Mount Sinai West, NY, USA.

⁸Department of Environment Medicine, NYU School of Medicine, New York, NY, USA

*Co-corresponding author

Contact: catarina.hioe@mssm.edu, catarina.hioe@va.gov

Summary of main points (40 words): IgM, IgG1 and IgA1 antibodies against SARS-CoV-2 spike

glycoprotein and its receptor-binding domain are present in convalescent COVID-19 plasma. Like IgG,

IgM and IgA contribute to virus neutralization, providing the basis for optimal selection of convalescent

plasma for COVID-19 treatment.

26 **Footnotes:**

27 ^aThis study was supported by the Microbiology Laboratory Clinical Services at the Mount Sinai Health
28 System and the Mount Sinai Health System Translational Science Hub; the Department of Medicine of the
29 Icahn School of Medicine at Mount Sinai Department of Medicine (to S.Z-P., C.E.H.); the Department of
30 Microbiology and the Ward-Coleman estate for endowing the Ward-Coleman Chairs at the Icahn School
31 of Medicine at Mount Sinai (to B.L.), the Department of Veterans Affairs [Merit Review Grant
32 I01BX003860] (to C.E.H.) and [Research Career Scientist Award 1IK6BX004607] (to C.E.H.); the
33 National Institutes of Health [grant AI139290] to C.E.H., [grants R01 AI123449, R21 AI1498033] to B.L,
34 and [grant U54TR001433]. K.Y.O. and C.S. were supported by Viral-Host Pathogenesis Training Grant
35 T32 AI07647; K.Y.O. was additionally supported by F31 AI154739. S.I. and C-T. H. were supported by
36 postdoctoral fellowships from CHOT-SG (Fukuoka University, Japan) and the Ministry of Science and
37 Technology (MOST, Taiwan), respectively.

38
39 ^bThe authors declare no competing interests.

40
41 *Co-corresponding author

42 Contact: catarina.hioe@mssm.edu, catarina.hioe@va.gov

43

44 **Abstract – 160 words**

45 **Background:** SARS-CoV-2 has infected millions of people globally. Virus infection requires the
46 receptor-binding domain (RBD) of the spike protein. Although studies have demonstrated anti-spike and -
47 RBD antibodies to be protective in animal models, and convalescent plasma as a promising therapeutic
48 option, little is known about immunoglobulin (Ig) isotypes capable of blocking infection.

49 **Methods:** We studied spike- and RBD-specific Ig isotypes in convalescent and acute plasma/sera using a
50 multiplex bead assay. We also determined virus neutralization activities in plasma, sera, and purified Ig
51 fractions using a VSV pseudovirus assay.

52 **Results:** Spike- and RBD-specific IgM, IgG1, and IgA1 were produced by all or nearly all subjects at
53 variable levels and detected early after infection. All samples displayed neutralizing activity. Regression
54 analyses revealed that IgM and IgG1 contributed most to neutralization, consistent with IgM and IgG
55 fractions' neutralization potency. IgA also exhibited neutralizing activity, but with lower potency.

56 **Conclusion:** IgG, IgM and IgA are critical components of convalescent plasma used for COVID-19
57 treatment.

58

59 **Keywords**

60 SARS-CoV-2, COVID-19, antibody isotypes, neutralization, convalescent plasma

61 **Text – 3499 words**

62 **Background**

63 Since the first patients with coronavirus disease 2019 (COVID-19), caused by severe acute
64 respiratory syndrome coronavirus 2 (SARS-CoV-2), were identified in Wuhan, China [1], the epidemic
65 has spread worldwide, infecting millions of people. Effective therapeutics and vaccines are urgently
66 needed. Convalescent plasma transfusions have shown promising results in patients with severe COVID-
67 19 [2–4] and clinical trials to evaluate its efficacy for ambulatory and hospitalized patients are underway
68 [5–7]. To this end, information is needed about immunoglobulin (Ig) isotypes in convalescent plasma that
69 have antiviral activities. The data would likewise inform vaccine development [8]. Most vaccines are
70 based on the SARS-CoV-2 spike protein [8,9], which is a membrane-anchored protein present on the virus
71 envelope along with two others (membrane and envelope proteins) and contains the receptor-binding
72 domain (RBD) for binding and entry into cells [10–12]. The vaccines aim to protect by inducing
73 neutralizing antibodies (Abs) that block viral infection.

74 SARS-CoV-2 spike-, RBD- and nucleocapsid-specific serum and plasma Abs of IgM, IgG, and
75 IgA isotypes are found in most COVID-19 patients [13–18], with neutralizing activities developing within
76 two weeks of infection and declining over time [15,16,19,20]. However, the neutralizing titers vary greatly
77 [15,16,19,20] and correlate with Ab binding levels against RBD, spike, and/or nucleocapsid, and with age,
78 symptom duration, and symptom severity [15,16]. Several RBD-specific monoclonal IgG Abs with
79 neutralizing activity have been generated, and these confer protection in animal models [15,19,21,22]. A
80 monoclonal Ab of IgA isotype recognizing both SARS-CoV-1 and SARS-CoV-2 spike proteins and
81 blocking ACE2 receptor binding was recently described [23]. However, no direct evidence is available
82 regarding the neutralizing capacity of plasma IgM and IgA from COVID-19 patients.

83 Studies on other respiratory viruses such as influenza show that, in addition to IgG, IgA could also

84 mediate virus neutralization, and their relative contribution depends on the physiologic compartment in
85 which they are found, with IgA contributing to the protection of mostly the upper respiratory tract while
86 IgG was protecting the lower respiratory tract [24,25]. An anti-hemagglutinin monoclonal polymeric IgA
87 has been demonstrated to mediate more potent anti-influenza activities than monoclonal IgG against the
88 same epitope [26]. An IgM monoclonal Ab with neutralizing activity against influenza B has also been
89 described [27]. In addition, respiratory syncytial virus (RSV)-specific mucosal IgA are a better correlate
90 of protection than serum IgG counterparts [28]. In the case of SARS-CoV-1, high titers of IgA in the lungs
91 correlated with reduced pathology in animal models [29]. Whether IgA in the blood and the respiratory
92 tract mucosa offer protection against SARS-CoV-2 remains an open question. Moreover, scant data are
93 available regarding IgM contribution to neutralization and protection against viruses, including SARS-
94 CoV-2. Of note, in terminally ill patients, systemic SARS-CoV-2 infection affects multiple organs [30].
95 Thus, the capacity of plasma Ig to suppress virus spread is critical for effective therapy against severe
96 COVID-19.

97 We recently described a multiplex bead Ab-binding assay using the Luminex technology to detect
98 total Ig against spike and RBD [31]. Here we characterized the Ig isotype profiles using the Luminex
99 assay that detects spike- and RBD-specific IgM, IgG1-4, and IgA1-2. Using a pseudovirus assay [32], we
100 also measured plasma or serum neutralization and determined the neutralizing capacity of IgM, IgA, and
101 IgG fractions. The data indicate a high prevalence of spike- and RBD-specific IgM and IgA, similar to that
102 of IgG1, in plasma and sera from COVID-19 patients, and their contributions to virus neutralization. In
103 addition, by testing purified IgG, IgM and IgA fractions from convalescent plasma, this study presents the
104 first direct evidence that plasma IgG, IgM, and IgA all contribute to SARS-CoV-2 neutralization.

105 **Methods**

106 **Recombinant proteins.** SARS-CoV-2 spike and RBD proteins were produced as described
107 [33,34].

108 **Human samples.** All COVID-19-positive and -negative samples tested in this study are tabulated
109 in **Supplementary Table 1**. Twenty-five citrated COVID-19 convalescent plasma samples destined for
110 transfusion to SARS-CoV-2-infected individuals (TF#1-25, collected between March 26th and April 7th
111 2020) and ten contemporary COVID-19-negative specimens (N#4-13) were obtained from the Division of
112 Transfusion Medicine of the Department of Pathology, Molecular and Cell-Based Medicine (Mount Sinai
113 Hospital System, IRB #20-03574). The convalescent specimens TF#1-25 were from donors pre-screened
114 to have serum IgG reciprocal titer ≥ 320 in the Mount Sinai Hospital ELISA anti-IgG COVID-19 assay.
115 Four sera from de-identified COVID-19 individuals (P#5-8) were provided by the Clinical Pathology
116 Division of the Department of Pathology, Molecular and Cell-Based Medicine at the Icahn School of
117 Medicine at Mount Sinai. The following samples were obtained from volunteers enrolled in IRB-approved
118 protocols at the Icahn School of Medicine at Mount Sinai (IRB #16-00772, #16-00791, #17-01243) and
119 the James J. Peter Veterans Affairs Medical Center (IRB #BAN-1604): sera from seven participants with
120 documented SARS-CoV-2 infection (P#1 d8, d11, and d15 after symptom onset, P#2 d7 and d10 after
121 symptom onset, and RP#1-5 after convalescence), and pre-pandemic sera from twelve healthy donors
122 (N#1-3, N#14-22). All study participants provided written consent. All samples were heat-inactivated
123 before use.

124 **Ig fractionation.** IgA was isolated first from plasma using peptide M agarose beads (InvivoGen
125 #GEL-PDM). The pass-through plasma was enriched sequentially for IgG using protein G agarose beads
126 (InvivoGen #GEL-AGG) and for IgM using a HiTrap IgM column (G.E. Healthcare #17-5110-01). An
127 additional step was performed using Protein A Plus mini-spin columns to separate IgG from IgM. Protein
128 concentrations were determined with Nanodrop (Thermo Scientific).

129 **Multiplex bead Ab binding assay.** SARS-CoV-2 spike and RBD antigens were coupled to beads
130 and experiments performed as described [31] except for the use of different secondary Abs designated in
131 the figure legends.

132 **COV2pp production and titration.** SARS-CoV-2 pseudoviruses (COV2pp) with wild-type (WT)
133 or D614G-mutated spike proteins were produced as described [32]. Pseudoviruses were titrated on 20,000
134 Vero-CCL81 cells seeded 24 hours before infection. At 18-22 hours post-infection, the infected cells were
135 washed and Renilla luciferase activity was measured with the Renilla-GloTM Luciferase Assay System
136 (Promega #E2720) on a Cytation3 (BioTek) instrument.

137 **COV2pp neutralization.** Virus was pre-incubated with diluted samples for 30 minutes. The virus-
138 sample mix was then added to Vero-CCL81 cells seeded 24 hours earlier and spinoculated. Infection was
139 measured after 18-22 hours by luciferase activity.

140 The percentage of neutralization was calculated as follows: $100 - ([\text{sample RLU} - \text{cell control RLU}] / \text{virus control RLU}) * 100$. IC₅₀ and IC₉₀ titers were calculated as the reciprocal sample dilution or
141 purified Ig fraction concentration achieving 50% and 90% neutralization, respectively.

142 **Statistical analysis.** Two-tailed Mann-Whitney test, Spearman rank-order correlation test, and
143 simple linear regressions were performed as designated in the figure legends using GraphPad Prism 8.

145 **Results**

146 **Levels of Ig isotypes against the SARS-CoV-2 spike and RBD vary in convalescent**
147 **individuals.** A total of 29 serum (P#5-8) and plasma (TF#1-25) specimens from COVID-19 convalescent
148 individuals was tested. TF#1-25 were collected ~4-8 weeks after the initial outbreak in North American,
149 and used for transfusion into hospitalized COVID-19 patients [2]. Ten plasma from COVID-negative
150 contemporaneous blood bank donors (N#4-13) were included for comparison. Sera or plasma from 12
151 uninfected individuals banked prior to the COVID-19 outbreak (N#1-3 and N#14-22) were used to
152 establish background values. The specimens were initially titrated for total Ig against spike and RBD (**Fig.**
153 **1**). All 29 COVID-19 positive specimens exhibited titration curves of total Ig Abs against spike, while
154 none of the negative controls displayed reactivity. Similar results were observed with RBD, except that
155 one contemporaneous COVID-19-negative sample had a low level of RBD-specific Ig (N#10). Overall,

156 the background MFI values were higher for RBD than spike. To assess the reproducibility of the assay, the
157 samples were tested in at least two separate experiments run on different days, and a strong correlation
158 was observed between the MFI values from these independent experiments (**Supplementary Fig. 1**). The
159 areas under the curves (AUCs) highly correlated with the MFI values from specimens diluted 1:200 (p
160 <0.0001 ; **Supplementary Fig. 2**); consequently, all samples were tested for isotyping at this dilution. At
161 the 1:200 dilution we were able to discern a diverse range of Ig isotype levels among individual samples
162 (**Fig. 2**). To evaluate for the presence of spike-specific and RBD-specific total Ig, IgM, IgG1, IgG2, IgG3,
163 IgG4, IgA1 and IgA2, the specificity and strength of the secondary Abs used to detect the different
164 isotypes were first validated with Luminex beads coated with myeloma proteins of known Ig isotypes
165 (IgG1, IgG2, IgG3, IgG4, IgA1, IgA2, and IgM). All eight secondary Abs were able to detect their
166 specific Ig isotypes with MFI values reaching $>60,000$ (**Supplementary Fig. 3**).

167 All 29 convalescent individuals had anti-spike and anti-RBD total Ig (**Fig. 2**), but the Ig levels
168 were highly variable, with MFI values ranging from 36,083 to 190,150. In addition, all 29 convalescent
169 individuals also displayed IgM Abs against spike at varying levels, and 93% were positive for anti-RBD
170 IgM when evaluated using cut-off values calculated as mean + 3 standard deviation (SD) of the 12 pre-
171 pandemic samples (**Fig 2b, c**). An IgG1 response was detected against both spike and RBD in 97% of the
172 convalescent subjects, with MFI values that ranged from 1,013 to 59,880. In contrast, IgG2, IgG3, and
173 IgG4 Abs against spike and RBD were detected in only a small fraction of the subjects, and the levels
174 were very low (MFI $<1,300$) (**Fig. 2**). Surprisingly, almost all individuals produced IgA1 Abs against
175 spike (97%) and RBD (93%), while 17% exhibited IgA2 against spike, and 48% exhibited IgA2 against
176 RBD (**Fig. 2**). Low levels, slightly above cut-off, of spike- and RBD-binding total Ig, IgM, IgG1, and
177 IgA1 were detected sporadically in contemporaneous COVID-19 samples, such as N#8, N#10, and N#11.
178 The responses against spike and RBD were highly correlated for every isotype (**Supplementary Fig. 4**).
179 Overall, these data demonstrate that IgM, IgG1, and IgA1 Abs were induced against spike and RBD in all

180 or almost all COVID-19 convalescent individuals (**Fig. 2**). The levels, however, were highly variable
181 among individuals. No significant difference was observed between female and male individuals
182 (**Supplementary Fig. 5**).

183 In **Fig. 3**, regression analyses to assess the impact of individual isotypes on the total Ig binding
184 showed that IgG1 had the highest r^2 values (0.83 and 0.70 for spike- and RBD-binding IgG1, respectively)
185 with $p < 0.0001$, indicating that IgG1 is the major isotype induced by SARS-CoV-2 infection against spike
186 and RBD (**Fig. 3a,b**). IgG2 Abs against RBD had an r^2 value of 0.55 with $p < 0.0001$, but IgG2 levels were
187 very low. For all other isotypes, including IgM, the r^2 values were < 0.40 (**Fig. 3c**). Thus, despite the
188 presence of many isotypes in sera and plasma, as expected, the major isotype of spike and RBD-specific
189 Abs is IgG1.

190 Specimens from two patients (P#1 and P#2) were drawn during the acute phase of the infection.
191 Serial specimens from these patients were tested to determine the isotypes of Abs present early in
192 infection. The earliest samples from both patients, drawn at 7 or 8 days after symptom onset were already
193 positive for total Ig, IgG1, IgA1 and IgM Abs against spike and RBD (**Supplementary Fig. 6**), and these
194 levels increased over the following three to seven days. On the contrary, IgA2 Ab levels were near or
195 below background on days 7-8 and remained unchanged over the two weeks post-onset. IgG4 Abs also
196 remained low or near background, whereas IgG2 and IgG3 Abs increased slightly to above background
197 after 10-15 days.

198 **Neutralizing activity is detected in specimens from all convalescent COVID-19 individuals.**

199 We subsequently tested the ability of samples from convalescent subjects to neutralize a VSV Δ G
200 pseudovirus bearing the SARS-CoV-2 spike protein (COV2pp). This pseudovirus assay demonstrated a
201 strong positive correlation with neutralization of the authentic SARS-CoV-2 virus [32]. The titration of
202 neutralizing activity against the WT COV2pp is shown in **Fig. 4a** for specimens from 28 COVID-19
203 convalescent individuals and 11 uninfected individuals, tested over a range of seven serial four-fold

204 dilutions. A soluble recombinant RBD (sRBD) protein capable of blocking virus infection was tested in
205 parallel as a positive control.

206 All specimens from COVID-19 convalescent individuals were able to neutralize the virus at levels
207 above 50% (**Fig. 4a**). For 26 of 28 specimens, neutralization reached >90% (**Fig. 4a**). The sample with the
208 lowest titer (reciprocal IC₅₀ titer = 37) reached a neutralization plateau of only ~60%. Of note, one sample
209 (TF#11) demonstrated highly potent neutralization with a reciprocal IC₅₀ titer > 40,960, and neutralization
210 was still 75% at the highest dilution tested. None of the samples from uninfected individuals reached 50%
211 neutralization (**Fig. 4a**), while the sRBD positive control demonstrated potent neutralization with an IC₅₀
212 of 0.06 µg/mL (**Fig. 4a**), similar to that recently reported [32].

213 The samples were also tested for neutralization against a COV2pp bearing the spike with a D614
214 mutation (D614G mutant), as the D614G variant has become the most prevalent circulating strain in the
215 global pandemic [35]. Similar to the WT COV2pp, all COVID-19-convalescent samples had neutralizing
216 activity reaching >50%, while none of the negative samples did (**Fig. 4b**). The IC₉₀ titers against WT and
217 D614 mutant differed on average by only 1.7-fold and correlated strongly with each other (p<0.0001, **Fig.**
218 **4c**).

219 **IgM and IgG1 contribute most to SARS-CoV-2 neutralization.** Given our observation that Ab
220 isotype levels and neutralization titers varied tremendously among convalescent COVID-19 individuals
221 (**Figs. 2 and 5**), we investigated the relative contribution of each Ab isotype to the neutralizing activities.
222 Regression analyses were performed on 27 COVID-19 convalescent samples (TF#11 was excluded due to
223 its outlier neutralization titer). As expected, relatively high r² values (0.32–0.62) and significant p values
224 were observed with total Ig, IgM and IgG1; in each case, r² values were higher for spike than for RBD
225 (**Fig. 6a**). The highest r² value was achieved in the analysis of IC₉₀ neutralizing titers and IgM binding to
226 spike (r²=0.62). For other isotypes, significant p values were sporadically achieved, but r² values were
227 weak (**Fig. 6a,b**).

228 **Neutralizing activities are mediated by plasma IgM, IgG, and IgA fractions.** To assess directly
229 the capacity of different isotypes to mediate neutralization, we evaluated the neutralization activities of
230 IgM, IgG, and IgA fractions purified from the plasma of five COVID-19 convalescent individuals (RP#1-
231 5). The enrichment of IgM, IgG1, and IgA1 Abs reactive with spike and RBD was validated using the
232 isotyping method used above (**Supplementary Fig. 7** and data not shown). These IgM, IgG, and IgA
233 fractions were then evaluated for neutralizing activity along with the original plasma (**Fig. 7**). The RP#1-5
234 plasma neutralizing reciprocal IC₅₀ titers ranged from 35 to 690 (**Fig. 7a,b**). Purified IgM and IgG
235 fractions from RP#1-5 all mediated neutralization reaching more than 50%. Unexpectedly, plasma IgA
236 fractions also displayed neutralizing activity, although not with the same potency as IgM and IgG (**Fig**
237 **7c,d**). In contrast, IgM, IgG, and IgA fractions from the negative control (RN#1) showed no neutralization
238 (**Fig. 7c,d**).

239 **Discussion**

240 Our study demonstrates that IgG1, IgA1 and IgM Abs against SARS-CoV-2 spike and RBD were
241 prevalent in plasma of convalescent COVID-19 patients approximately one to two months after infection.
242 These isotypes were present within 7-8 days after the onset of symptoms. Importantly, all three isotypes
243 showed the capacity to mediate virus neutralization. While regression analyses demonstrated the strongest
244 contributions of IgM and IgG1 to neutralizing activity, direct testing of purified isotype fractions showed
245 that IgA also were able to neutralize, indicating the protective potential of all three major Ig isotypes.
246 These data carry important implications for the use of convalescent plasma and hyperimmunoglobulin as
247 COVID-19 therapeutics, suggesting that their selection would optimally be based on the presence of all of
248 these Ig isotypes.

249 While all COVID-19 convalescent individuals exhibited neutralization activities reaching >50%
250 and 26 of 28 specimens attained 90% neutralization, neutralization levels were highly variable with IC₅₀
251 and IC₉₀ titers ranging over three orders of magnitude. The titers were comparable against the initial

252 Wuhan strain and the currently prevalent D614G strain of SARS-CoV-2. Similarly, the levels of spike-
253 and RBD-binding total Ig and Ig isotypes varied greatly.

254 A trend toward higher levels of total Ig and each Ig isotype was seen in female compared to male
255 subjects, as reported in another study [36]. Moreover, except for TF#11 (a male elite neutralizer), the
256 median neutralizing IC₉₀ titer was higher in females than males, although the difference did not reach
257 significance (data not shown). Sex differences in Ab induction have been observed following influenza
258 vaccination in humans and mice and were shown to result from the impact of sex-related steroids [37].
259 Whether and to what extent this contributes to the sex differences seen in clinical outcomes of COVID-19
260 remains to be investigated. Other studies have shown that Ab levels were associated with multiple factors,
261 including time from disease onset [38] and disease severity [14]. However, other than sex, clinical data are
262 not available for the subjects studied here, limiting our analysis only to neutralization and Ig isotypes.

263 One remarkable finding from our study is that although neutralization titers correlated with binding
264 levels of IgM and IgG1 and not with those of IgA1 or IgA2, purified IgA fractions from convalescent
265 COVID-19 patients exhibited significant neutralizing activities. The importance of this finding is
266 underscored by the data showing that IgA1 was the prominent isotype in some samples such as TF#7 and
267 TF#24 and that IgA1 could be detected early after symptom onset. Data from other studies also support
268 the significance of IgA in that purified IgA fractions exhibited more, or as potent neutralizing activities as
269 purified IgG, and that RBD-binding IgA correlated as strongly as IgG with micro-neutralization titers
270 [39]. IgA were also detected in saliva and bronchoalveolar lavage from COVID-19 patients [40].
271 Nonetheless, Wang *et al.* reported that plasma IgA monomers were less potent than the plasma IgG and
272 secretory IgA counterparts [41]. In our study, neutralization activities detected in the IgA fractions were
273 mediated mainly by IgA1, the predominant IgA isotype in plasma, and the IC₅₀ potency of the IgA
274 fraction was ~4-fold lower than the potency of IgM and IgG1 fractions. This difference cannot be
275 explained entirely by lower amounts of spike-specific IgA1 in the tested fractions, as estimations using

276 spike-specific monoclonal IgA and IgM Abs yielded similar IgA and IgM concentrations in the respective
277 purified fractions (median of 2 and 2.5 µg/mL respectively). Fine epitope specificities and affinities may
278 differ for IgA, IgM, and IgG to impact neutralization potency, but have yet to be evaluated.

279 In addition to neutralization, non-neutralizing Ab activities have been implicated in protection
280 from various virus infection through potent Fc-mediated functions such as antibody-dependent cellular
281 cytotoxicity (ADCC), antibody-dependent cellular phagocytosis (ADCP), and complement-mediated lysis;
282 this is reported for HIV, influenza, Marburg, and Ebola viruses [25,42–44]. The Fc activities were not
283 evaluated in our study, and their contribution to protection against SARS-CoV-2 is yet unclear [45,46]. A
284 recent study demonstrated enrichment of spike-specific IgM and IgA1 Abs and spike-specific phagocytic
285 and antibody-dependent complement deposition (ADCD) activity in plasma of individuals who recovered
286 from SARS-CoV-2 infection, while nucleocapsid-specific IgM and IgA2 responses and nucleocapsid-
287 specific ADCD activity were features enriched in deceased patients [47]. DNA vaccines expressing full-
288 length and truncated spike proteins could curtail SARS-CoV-2 infection in the respiratory tract by varying
289 degrees in rhesus macaques. This virus reduction correlated with levels of neutralization and also with Fc-
290 mediated effector functions such as ADCD [45]. Interestingly, these DNA vaccines elicited spike- and
291 RBD-specific IgG1, IgG2, IgG3, IgA, and IgM Abs, and similar to our findings, neutralization correlated
292 most strongly with IgM. Adenovirus serotype 26 vaccine vectors encoding seven SARS-CoV-2 spike
293 variants also showed varying protection levels, and virus reduction correlated best with neutralizing titers
294 together with IgM binding levels, FcγRII-binding, and ADCD responses [48]. Defining the full functional
295 potential of Abs against SARS-CoV-2—including neutralizing, non-neutralizing, and enhancing
296 activities—are vital for determining the optimal Ab treatment modalities against COVID-19 and the
297 potential efficacy of COVID-19 vaccine candidates.

298 When we examined plasma specimens collected within 7-8 days after COVID-19 symptom onset,
299 we detected IgG and IgA against spike and RBD, as well as IgM. This is consistent with published reports

300 showing that 100% of COVID-19-infected individuals developed IgG within 19 days after symptom onset
301 and that IgG and IgM seroconversion could occur simultaneously [14]. IgA were also found early after
302 infection (4-6 days after symptom onset) and increased over time [13,18,40]. These studies suggest that
303 measuring total Ig, rather than IgG, could contribute to improved outcomes for early disease diagnosis.
304 We found no correlation between the levels of different isotypes in the specimens examined in our study
305 (data not shown). Of note, IgA presence early during acute infection may suggest the potential
306 contribution of natural IgA, which, similar to natural IgM, arises spontaneously from innate B1 cells to
307 provide the initial humoral responses before the induction of adaptive classical B cells [49].

308 In summary, this study demonstrates that spike- and RBD-specific IgM, IgG1, and IgA1 are
309 produced by all or almost all analyzed COVID-19 convalescent subjects and can be detected at early
310 stages of infection. The plasma samples of convalescent individuals also display neutralization activities
311 mediated by IgM, IgG, and IgA1, although neutralization titers correlated more strongly with IgM and
312 IgG levels. The contribution of IgM, IgG, and IgA to SARS-CoV-2-neutralizing activities demonstrates
313 their importance in the efficacy of passively transferred Abs for SARS-CoV-2 treatment.

314

315 **References**

- 316 1. Zhu N, Zhang D, Wang W, et al. A Novel Coronavirus from Patients with Pneumonia in China,
317 2019. *N Engl J Med.* **2020**; 382(8):727–733.
- 318 2. Liu STH, Lin H-M, Baine I, et al. Convalescent plasma treatment of severe COVID-19: a
319 propensity score-matched control study. *Nat Med.* **2020**; .
- 320 3. Zeng H, Wang D, Nie J, et al. The efficacy assessment of convalescent plasma therapy for
321 COVID-19 patients: a multi-center case series. *Signal Transduct Target Ther.* Nature Publishing Group;
322 **2020**; 5(1):1–12.
- 323 4. Ibrahim D, Dulipsingh L, Zapatka L, et al. Factors Associated with Good Patient Outcomes

- 324 Following Convalescent Plasma in COVID-19: A Prospective Phase II Clinical Trial. *Infect Dis Ther.*
325 **2020**; :1–14.
- 326 5. Janssen M, Schäkel U, Fokou CD, et al. A Randomized Open label Phase-II Clinical Trial with or
327 without Infusion of Plasma from Subjects after Convalescence of SARS-CoV-2 Infection in High-Risk
328 Patients with Confirmed Severe SARS-CoV-2 Disease (RECOVER): A structured summary of a study
329 protocol for a randomised controlled trial. *Trials. BioMed Central*; **2020**; 21(1):1–4.
- 330 6. Convalescent Plasma to Limit SARS-CoV-2 Associated Complications - Full Text View -
331 ClinicalTrials.gov [Internet]. [cited 2020 Nov 2]. Available from:
332 <https://clinicaltrials.gov/ct2/show/NCT04373460>
- 333 7. Convalescent Plasma in Outpatients With COVID-19 - Full Text View - ClinicalTrials.gov
334 [Internet]. [cited 2020 Nov 2]. Available from: <https://clinicaltrials.gov/ct2/show/NCT04355767>
- 335 8. Le TT, Andreadakis Z, Kumar A, et al. The COVID-19 vaccine development landscape. *Nat Rev*
336 *Drug Discov. Nature Publishing Group*; **2020**; 19(5):305–306.
- 337 9. Amanat F, Krammer F. SARS-CoV-2 Vaccines: Status Report. *Immunity*. **2020**; .
- 338 10. Yan R, Zhang Y, Li Y, Xia L, Guo Y, Zhou Q. Structural basis for the recognition of SARS-CoV-
339 2 by full-length human ACE2. *Science*. **2020**; 367(6485):1444–1448.
- 340 11. Hoffmann M, Kleine-Weber H, Schroeder S, et al. SARS-CoV-2 Cell Entry Depends on ACE2
341 and TMPRSS2 and Is Blocked by a Clinically Proven Protease Inhibitor. *Cell*. **2020**; 181(2):271-280.e8.
- 342 12. Walls AC, Park Y-J, Tortorici MA, Wall A, McGuire AT, Velesler D. Structure, Function, and
343 Antigenicity of the SARS-CoV-2 Spike Glycoprotein. *Cell*. **2020**; 181(2):281-292.e6.
- 344 13. Ma H, Zeng W, He H, et al. Serum IgA, IgM, and IgG responses in COVID-19. *Cell Mol*
345 *Immunol. Nature Publishing Group*; **2020**; 17(7):773–775.
- 346 14. Long Q-X, Liu B-Z, Deng H-J, et al. Antibody responses to SARS-CoV-2 in patients with
347 COVID-19. *Nat Med. Nature Publishing Group*; **2020**; 26(6):845–848.

- 348 15. Robbiani DF, Gaebler C, Muecksch F, et al. Convergent antibody responses to SARS-CoV-2 in
349 convalescent individuals. *Nature*. **2020**; .
- 350 16. Okba NMA, Müller MA, Li W, et al. Severe Acute Respiratory Syndrome Coronavirus 2-Specific
351 Antibody Responses in Coronavirus Disease Patients. *Emerg Infect Dis*. **2020**; 26(7):1478–1488.
- 352 17. Guo L, Ren L, Yang S, et al. Profiling Early Humoral Response to Diagnose Novel Coronavirus
353 Disease (COVID-19). *Clin Infect Dis Off Publ Infect Dis Soc Am*. **2020**; .
- 354 18. Padoan A, Sciacovelli L, Basso D, et al. IgA-Ab response to spike glycoprotein of SARS-CoV-2 in
355 patients with COVID-19: A longitudinal study. *Clin Chim Acta*. **2020**; 507:164–166.
- 356 19. Ju B, Zhang Q, Ge J, et al. Human neutralizing antibodies elicited by SARS-CoV-2 infection.
357 *Nature*. **2020**; .
- 358 20. Prévost J, Gasser R, Beaudoin-Bussièrès G, et al. Cross-Sectional Evaluation of Humoral
359 Responses against SARS-CoV-2 Spike. *Cell Rep Med*. **2020**; 1(7):100126.
- 360 21. Rogers TF, Zhao F, Huang D, et al. Isolation of potent SARS-CoV-2 neutralizing antibodies and
361 protection from disease in a small animal model. *Science* [Internet]. American Association for the
362 Advancement of Science; **2020** [cited 2020 Jul 16]; . Available from:
363 <https://science.sciencemag.org/content/early/2020/06/15/science.abc7520>
- 364 22. Zost SJ, Gilchuk P, Case JB, et al. Potently neutralizing and protective human antibodies against
365 SARS-CoV-2. *Nature*. Nature Publishing Group; **2020**; :1–10.
- 366 23. Ejemel M, Li Q, Hou S, et al. IgA MAb blocks SARS-CoV-2 Spike-ACE2 interaction providing
367 mucosal immunity. *BioRxiv Prepr Serv Biol*. **2020**; .
- 368 24. Renegar KB, Small PA, Boykins LG, Wright PF. Role of IgA versus IgG in the control of
369 influenza viral infection in the murine respiratory tract. *J Immunol Baltim Md 1950*. **2004**; 173(3):1978–
370 1986.
- 371 25. Krammer F. The human antibody response to influenza A virus infection and vaccination. *Nat Rev*

- 372 Immunol. **2019**; 19(6):383–397.
- 373 26. Muramatsu M, Yoshida R, Yokoyama A, et al. Comparison of antiviral activity between IgA and
374 IgG specific to influenza virus hemagglutinin: increased potential of IgA for heterosubtypic immunity.
375 PloS One. **2014**; 9(1):e85582.
- 376 27. Shen C, Zhang M, Chen Y, et al. An IgM antibody targeting the receptor binding site of influenza
377 B blocks viral infection with great breadth and potency. *Theranostics*. **2019**; 9(1):210–231.
- 378 28. Habibi MS, Jozwik A, Makris S, et al. Impaired Antibody-mediated Protection and Defective IgA
379 B-Cell Memory in Experimental Infection of Adults with Respiratory Syncytial Virus. *Am J Respir Crit*
380 *Care Med*. **2015**; 191(9):1040–1049.
- 381 29. Du L, He Y, Zhou Y, Liu S, Zheng B-J, Jiang S. The spike protein of SARS-CoV--a target for
382 vaccine and therapeutic development. *Nat Rev Microbiol*. **2009**; 7(3):226–236.
- 383 30. Schurink B, Roos E, Radonic T, et al. Viral presence and immunopathology in patients with lethal
384 COVID-19: a prospective autopsy cohort study. *Lancet Microbe*. **2020**; .
- 385 31. Weiss S, Klingler J, Hioe C, et al. A High Through-put Assay for Circulating Antibodies Directed
386 against the S Protein of Severe Acute Respiratory Syndrome Corona virus 2. medRxiv. Cold Spring
387 Harbor Laboratory Press; **2020**; :2020.04.14.20059501.
- 388 32. Oguntuyo KY, Stevens CS, Hung C-T, et al. Quantifying absolute neutralization titers against
389 SARS-CoV-2 by a standardized virus neutralization assay allows for cross-cohort comparisons of
390 COVID-19 sera. medRxiv. Cold Spring Harbor Laboratory Press; **2020**; :2020.08.13.20157222.
- 391 33. Amanat F, Stadlbauer D, Strohmeier S, et al. A serological assay to detect SARS-CoV-2
392 seroconversion in humans. *Nat Med*. Nature Publishing Group; **2020**; :1–4.
- 393 34. Stadlbauer D, Amanat F, Chromikova V, et al. SARS-CoV-2 Seroconversion in Humans: A
394 Detailed Protocol for a Serological Assay, Antigen Production, and Test Setup. *Curr Protoc Microbiol*.
395 **2020**; 57(1):e100.

- 396 35. Korber B, Fischer WM, Gnanakaran S, et al. Tracking Changes in SARS-CoV-2 Spike: Evidence
397 that D614G Increases Infectivity of the COVID-19 Virus. *Cell*. **2020**; 182(4):812-827.e19.
- 398 36. Zeng F, Dai C, Cai P, et al. A comparison study of SARS-CoV-2 IgG antibody between male and
399 female COVID-19 patients: a possible reason underlying different outcome between gender. medRxiv.
400 Cold Spring Harbor Laboratory Press; **2020**; :2020.03.26.20040709.
- 401 37. Potluri T, Fink AL, Sylvia KE, et al. Age-associated changes in the impact of sex steroids on
402 influenza vaccine responses in males and females. *Npj Vaccines*. Nature Publishing Group; **2019**; 4(1):1–
403 12.
- 404 38. Long Q-X, Tang X-J, Shi Q-L, et al. Clinical and immunological assessment of asymptomatic
405 SARS-CoV-2 infections. *Nat Med*. Nature Publishing Group; **2020**; :1–5.
- 406 39. Mazzini L, Martinuzzi D, Hyseni I, et al. Comparative analyses of SARS-CoV-2 binding (IgG,
407 IgM, IgA) and neutralizing antibodies from human serum samples. bioRxiv. Cold Spring Harbor
408 Laboratory; **2020**; :2020.08.10.243717.
- 409 40. Isho B, Abe KT, Zuo M, et al. Persistence of serum and saliva antibody responses to SARS-CoV-2
410 spike antigens in COVID-19 patients. *Sci Immunol [Internet]*. Science Immunology; **2020** [cited 2020 Oct
411 9]; 5(52). Available from: <https://immunology.sciencemag.org/content/5/52/eabe5511>
- 412 41. Wang Z, Lorenzi JCC, Muecksch F, et al. Enhanced SARS-CoV-2 Neutralization by Secretory
413 IgA in vitro. bioRxiv. Cold Spring Harbor Laboratory; **2020**; :2020.09.09.288555.
- 414 42. Horwitz, Bar-On Y, Lu C-L, et al. Non-neutralizing Antibodies Alter the Course of HIV-1
415 Infection In Vivo. *Cell*. **2017**; .
- 416 43. Ilinykh PA, Huang K, Santos RI, et al. Non-neutralizing Antibodies from a Marburg Infection
417 Survivor Mediate Protection by Fc-Effector Functions and by Enhancing Efficacy of Other Antibodies.
418 *Cell Host Microbe*. **2020**; 27(6):976-991.e11.
- 419 44. Gunn BM, Yu W-H, Karim MM, et al. A Role for Fc Function in Therapeutic Monoclonal

- 420 Antibody-Mediated Protection against Ebola Virus. *Cell Host Microbe*. **2018**; 24(2):221-233.e5.
- 421 45. Yu J, Tostanoski LH, Peter L, et al. DNA vaccine protection against SARS-CoV-2 in rhesus
422 macaques. *Science*. **2020**; .
- 423 46. Zohar T, Alter G. Dissecting antibody-mediated protection against SARS-CoV-2. *Nat Rev*
424 *Immunol*. **2020**; 20(7):392–394.
- 425 47. Atyeo C, Fischinger S, Zohar T, et al. Distinct Early Serological Signatures Track with SARS-
426 CoV-2 Survival. *Immunity* [Internet]. **2020** [cited 2020 Aug 12]; . Available from:
427 <http://www.sciencedirect.com/science/article/pii/S1074761320303277>
- 428 48. Mercado NB, Zahn R, Wegmann F, et al. Single-shot Ad26 vaccine protects against SARS-CoV-2
429 in rhesus macaques. *Nature*. **2020**; .
- 430 49. Meyer-Bahlburg A. B-1 cells as a source of IgA. *Ann N Y Acad Sci*. **2015**; 1362:122–131.
- 431
- 432

433 **Acknowledgments**

434 We thank Dr. Florian Krammer, Dr. Viviana Simon, and Dr. Rebecca Powell for donation of samples and
435 reagents, and all the donors for their contribution to the research.

436

437 **Author contributions**

438 J.K., S.W., G.E-A., S.Z-P., and C.E.H. wrote and edited the manuscript. S.W., J.K., C.E.H., and S.Z-P.
439 designed the experiments. J.K., S.W., V.I., X.L. performed the experiments and collected the data. J.K.,
440 A.N., S.Z-P. and C.E.H. analyzed the data. K.Y.O., C.S., S.I., C-T.H., F.A., and B.L. provided protocols,
441 antigens, cells and pseudovirus stocks. G.E-A., I.B., S.A., J.C.B., E.M.K., J.S., S.L., D.J., and M.B-G.
442 provided specimens. All authors read and approved the final manuscript.

443 **Figure Legends**

444 **Fig. 1. Titration of SARS-CoV-2 spike and RBD total Ig in plasma or serum samples from COVID-**
445 **19 convalescent individuals.** Titration of (a) spike-specific or (b) RBD-specific total Ig from 29 COVID-
446 19 convalescent individuals, two acute COVID-19 patients with longitudinal samples, and 13 COVID-19
447 uninfected negative individuals. Specimens were diluted at 2-fold dilutions from 1:50 to 1:6,400.

448
449 **Fig. 2. Levels of Ig isotypes against the SARS-CoV-2 spike and RBD vary in plasma or serum**
450 **samples from COVID-19 convalescent individuals.** Total Ig, IgM, IgG1, IgG2, IgG3, IgG4, IgA1 and
451 IgA2 against (a) spike and (b) RBD in specimens from 29 COVID-19 convalescent individuals, 13
452 COVID-19 uninfected contemporaneous samples, and pre-pandemic controls were detected using the
453 following secondary Abs: rabbit biotinylated-anti-human total Ig (Abcam, catalog #ab97158) at 2 µg/mL,
454 mouse biotinylated-anti-human IgG1 Fc (Invitrogen #MH1515) at 4 µg/mL, mouse biotinylated-anti-
455 human IgG2 Fc (Southern Biotech #9060-08) at 1 µg/mL, mouse biotinylated-anti-human IgG3 Hinge
456 (Southern Biotech #9210-08) at 3 µg/mL, mouse biotinylated-anti-human IgG4 Fc (Southern Biotech
457 #9200-08) at 4 µg/mL, mouse biotinylated-anti-human IgA1 Fc (Southern Biotech #9130-08) at 4 µg/mL,
458 mouse biotinylated-anti-human IgA2 Fc (Southern Biotech #9140-08) at 4 µg/mL or goat biotinylated-
459 anti-human IgM (Southern Biotech #2020-08) at 3 µg/mL. The samples were tested at a dilution of 1:200
460 and data are shown as mean MFI + standard deviation (SD) of duplicate measurements from at least two
461 independent experiments. The pre-pandemic controls are shown as mean MFI + SD of 12 samples (Pre,
462 black bar). The horizontal red dotted line represents the cut-off value determined as the mean + 3 SD of 12
463 pre-pandemic samples for each of the isotypes. (c) Percentages of responders above the cut-off for each
464 spike- or RBD-specific Ig isotype.

465
466 **Fig. 3. IgG1 is the dominant isotype induced in COVID-19 convalescent individuals.** Simple linear

467 regression of (a) spike-specific or (b) RBD-specific total Ig levels versus IgM, IgG1 or IgG2 levels versus
468 (c) spike-specific and RBD-specific IgG3, IgG4, IgA1, and IgA2 levels from the 29 COVID-19-
469 convalescent individuals from Fig. 1. The dash lines represent 95% confidence intervals.

470

471 **Fig. 4. Neutralization activities are detected in all COVID-19 convalescent individuals.** Neutralization
472 of COV2pp with (a) WT or (b) D614G mutated spike proteins by samples from 28 COVID-
473 19convalescent individuals and 11 COVID-19 uninfected individuals. The neutralizing activity of
474 recombinant soluble RBD (sRBD) is shown as a positive control. Twenty-four hours before infection,
475 20,000 Vero-CCL81 cells/well were seeded. Virus (82.5 μ L/well) was pre-incubated with serially diluted
476 samples (27.5 μ L/well, 4-fold from 1:10 to 1:40,960) for 30 minutes at room temperature. The
477 virus/sample mix was then added to the cells and spinoculated by centrifugation (1250 rpm, 1 hour, room
478 temperature). Six virus-only and six medium-only wells were kept for each plate. After 18 to 22 hours at
479 37°C, infection was measured by luciferase activity. sRBD was tested as a positive control at 4-fold
480 dilutions from 100 to 0.02 μ g/mL. The data are shown as mean percentage of neutralization + SD of
481 triplicates. The extrapolated titration curves were generated using a nonlinear regression model in
482 GraphPad Prism (Inhibitor versus response – variable slope [four parameters], least squares regression).
483 The dotted horizontal lines highlight 50% neutralization. (c) Spearman correlation between the IC₉₀ titers
484 against COV2pp WT vs. D614G.

485

486 **Fig. 5. Summary of relative Ig isotype levels and neutralization titers.** Table showing sex (purple, F:
487 female, M: male), relative levels of spike-specific (green) and RBD-specific (blue) Ig isotypes (+: bottom
488 quartile, ++: second quartile, +++: third quartile, ++++: top quartile, -: non-responder) and reciprocal IC₅₀
489 and IC₉₀ neutralization titers against WT pseudovirus (orange) and D614G pseudovirus (red) of 29 plasma
490 samples from COVID-19 convalescent individuals. nd: not done.

491 **Fig. 6. IgM and IgG1 contribute most to SARS-CoV-2 neutralization.** Simple linear regression of
492 reciprocal IC_{90} neutralization titers of 27 COVID-19 convalescent individuals versus (a) spike-specific or
493 (b) RBD-specific total Ig, IgM, IgG1 and IgA1 Ab levels. The black dash lines show the 95% confidence
494 intervals. The dotted vertical red line represents the cut-off (mean of 12 pre-pandemic samples + 3 SD) for
495 each isotype from Fig. 1. (c) Statistical results of simple linear regression analyses of reciprocal IC_{90}
496 neutralization titers of 27 COVID-19 convalescent individuals versus spike-specific or RBD-specific Abs
497 levels for IgG2-4 and IgA2.

498

499 **Fig. 7. Purified IgM, IgG, and IgA fractions display neutralizing activities against SARS-CoV-2.** (a)
500 Neutralization of COV2pp by five COVID-19-infected individual plasma samples (RP#1-5) compared to
501 a specimen from a COVID-19 uninfected individual (RN#1, green filled circles). Plasma samples were
502 tested at 4-fold dilutions from 1:10 to 1:40,960 or 1:20 to 1:81,920. Data are shown as the mean
503 percentage of neutralization. The dotted horizontal lines highlight 50% and 90% neutralization. (b)
504 Reciprocal IC_{50} and IC_{90} neutralization titers of RP#1-5 plasma samples (c) Neutralization of COV2pp by
505 purified IgM, IgG, and IgA fractions from five COVID-19-infected individuals (RP#1-5) compared to a
506 control Ig fraction (gray open triangles). IgA was isolated first from plasma samples by mixing 1:2 diluted
507 plasma with peptide M agarose beads (600 μ L/28 mL plasma, InvivoGen #GEL-PDM) for 1.5 hours at
508 room temperature. After washing beads, IgA was eluted with a pH 2.8 buffer (Thermo Scientific #21004)
509 and neutralized with pH 9 Tris buffer. The pass-through plasma sample was collected for IgG enrichment
510 using protein G agarose beads (InvivoGen #GEL-AGG) and subsequently for IgM isolation using a
511 HiTrap IgM column (G.E. Healthcare #17-5110-01). An additional purification step was performed using
512 Protein A Plus mini-spin columns to separate IgG from IgM. The fractions were tested at 4-fold dilutions
513 from 500 to 0.02 μ g/mL. Data are shown as the mean percentage of neutralization. The dotted horizontal
514 lines highlight 50% neutralization. (d) IC_{50} of purified IgM, IgG, and IgA fractions from RP#1-5. The

515 statistical significance was determined by a two-tailed Mann-Whitney test (*: $p < 0.05$, **: $p < 0.01$).

516

517 **Supplementary Fig. 1.** Spearman correlations of (a) spike-specific or (b) RBD-specific total Ig MFI
518 values from two independent experiments to show the degree of assay reproducibility.

519

520 **Supplementary Fig. 2.** Spearman correlations of the area under the curves (AUCs) of (a) spike- or (b)
521 RBD-specific total Ig versus total Ig MFI values at a 1:200 dilution.

522

523 **Supplementary Fig. 3.** Isotyping validation was performed by coating Luminex beads with IgG1, IgG2,
524 IgG3, IgG4, IgA1, IgA2, and IgM myeloma proteins and detecting each with eight different secondary
525 Abs against total Ig, IgM, IgG1, IgG2, IgG3, IgG4, IgA1 and IgA2. The data are shown as mean MFI +
526 SD of duplicate.

527

528 **Supplementary Fig. 4.** Spearman correlations between spike-specific versus RBD-specific total Ig, IgM,
529 IgG1, IgG2, IgG3, IgG4, IgA1, or IgA2 MFI values.

530

531 **Supplementary Fig. 5.** Violin plots of (a) spike-specific or (b) RBD-specific total Ig, IgM, IgG1, and
532 IgA1 levels from nine COVID-19 convalescent female (F) and 15 male (M) subjects. The statistical
533 significance was determined by a two-tailed Mann-Whitney test (ns: non-significant: $p > 0.05$).

534

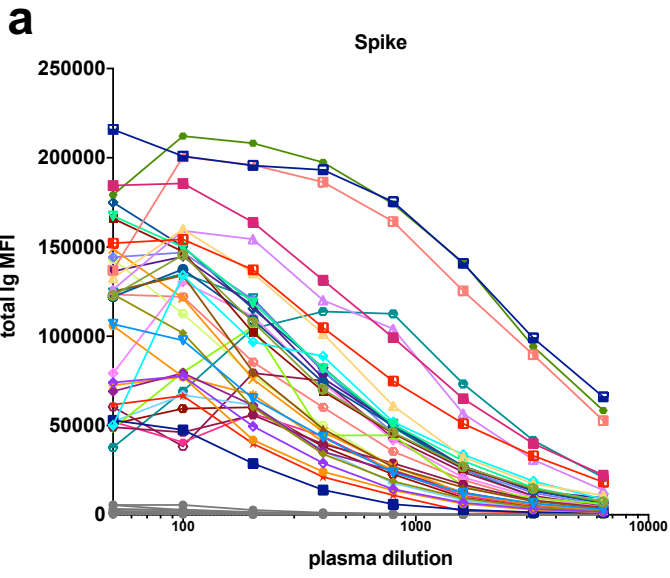
535 **Supplementary Fig. 6. Induction of IgA1 and IgG1 along with IgM early after disease onset.** Kinetics
536 of induction of spike-specific (left panel) or RBD-specific (right panel) total Ig, IgM, IgG1, IgG2, IgG3,
537 IgG4, IgA1, and IgA2 from two COVID-19 patients. Longitudinal samples from each patient were tested
538 at a dilution of 1:200 in parallel with all negative samples and data are shown as mean MFI + SD of

539 duplicate measurements from at least two experiments. The dotted red line represents the cut-off value
540 calculated as the mean of 12 pre-pandemic samples + 3 SD from Fig. 1.

541

542 **Supplementary Fig. 7. Enrichment of spike-specific (a) IgM, (b) IgG, and (c) IgA in purified**
543 **fractions from RP#1-5 and RN#1.** Each purified isotype fraction from plasma was measured for the
544 presence of IgM, IgG1, IgG2, IgG3, IgG4, IgA1, and IgA2 Abs using the isotyping method validated in
545 Supplementary Fig. 3.

546



- P#1a
- P#1b
- P#1c
- P#2a
- P#2b
- P#3
- P#4
- P#5
- P#6
- P#7
- P#8
- TF#1
- TF#2
- TF#3
- TF#4
- TF#5
- TF#6
- TF#7
- TF#8
- TF#9
- TF#10
- TF#11
- TF#12
- TF#13
- TF#14
- TF#15
- TF#16
- TF#17
- TF#18
- TF#19
- TF#20
- TF#21
- TF#22
- TF#23
- TF#24
- TF#25
- COVID-19-negative subjects

COVID-19-positive subjects

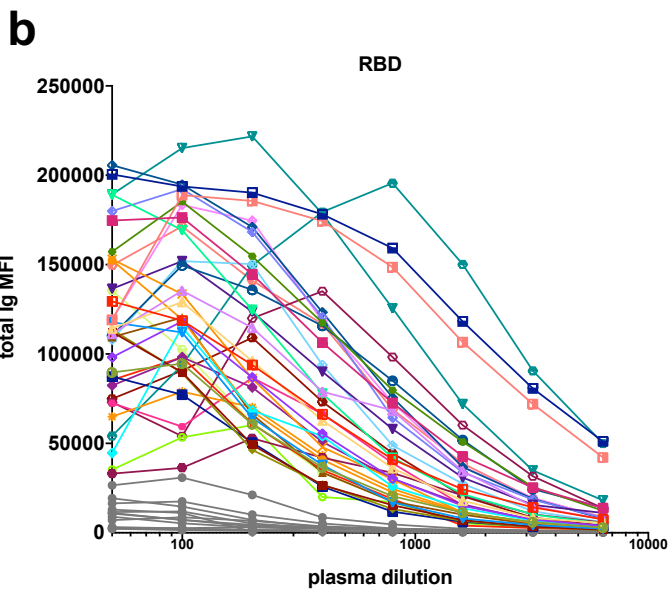
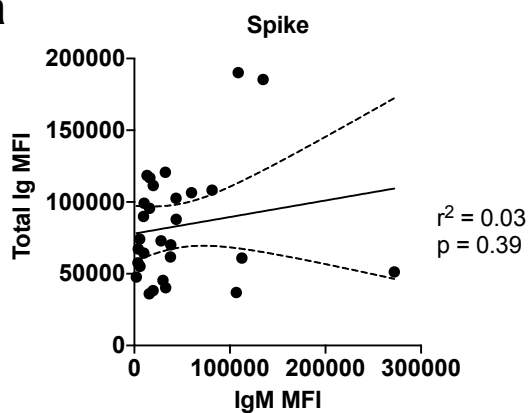
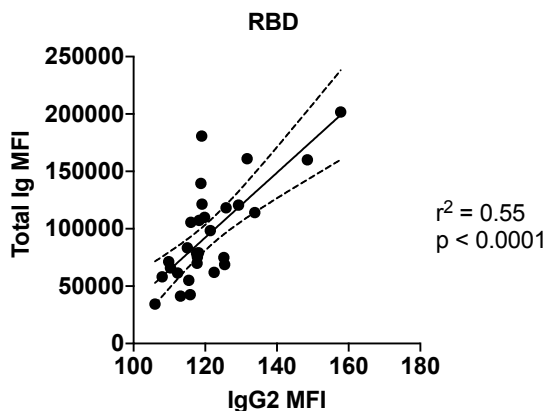
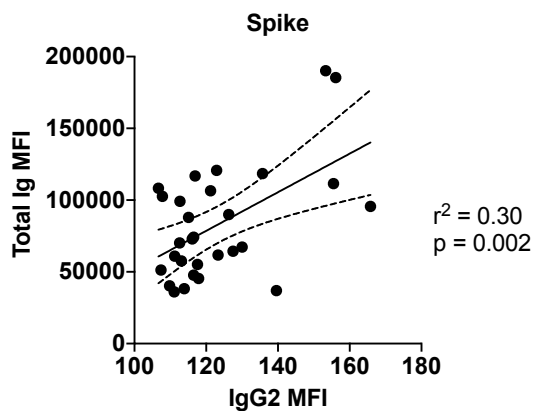
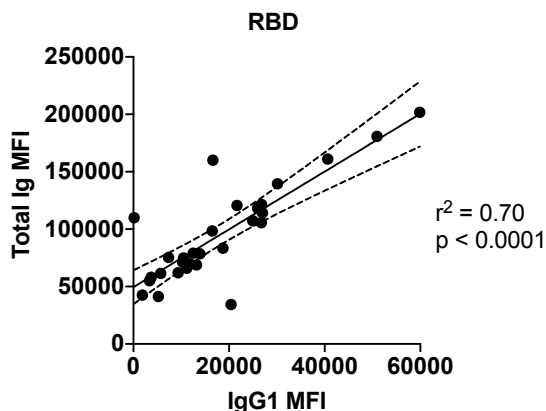
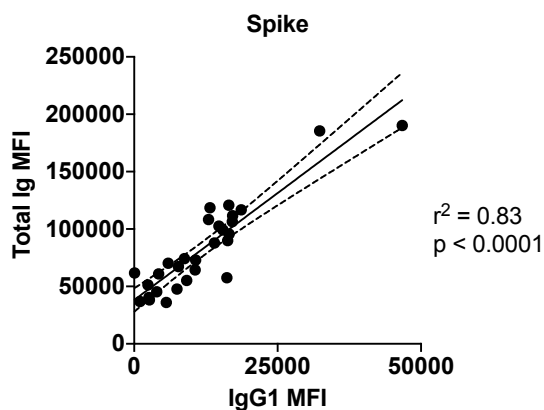
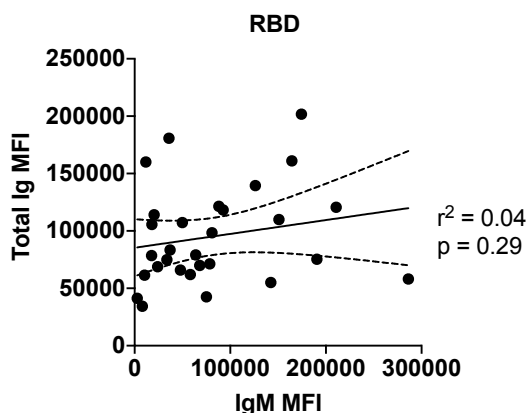


Fig. 1. Titration of SARS-CoV-2 spike and RBD total Ig in plasma or serum samples from COVID-19 convalescent individuals. Titration of (a) spike-specific or (b) RBD-specific total Ig from 29 COVID-19 convalescent individuals, two acute COVID-19 patients with longitudinal samples, and 13 COVID-19 uninfected negative individuals. Specimens were diluted at 2-fold dilutions from 1:50 to 1:6,400.

Fig. 2. Levels of Ig isotypes against the SARS-CoV-2 spike and RBD vary in plasma or serum samples from COVID-19 convalescent individuals. Total Ig, IgM, IgG1, IgG2, IgG3, IgG4, IgA1 and IgA2 against (a) spike and (b) RBD in specimens from 29 COVID-19 convalescent individuals, 13 COVID-19 uninfected contemporaneous samples, and pre-pandemic controls were detected using the following secondary Abs: rabbit biotinylated-anti-human total Ig (Abcam, catalog #ab97158) at 2 $\mu\text{g}/\text{mL}$, mouse biotinylated-anti-human IgG1 Fc (Invitrogen #MH1515) at 4 $\mu\text{g}/\text{mL}$, mouse biotinylated-anti-human IgG2 Fc (Southern Biotech #9060-08) at 1 $\mu\text{g}/\text{mL}$, mouse biotinylated-anti-human IgG3 Hinge (Southern Biotech #9210-08) at 3 $\mu\text{g}/\text{mL}$, mouse biotinylated-anti-human IgG4 Fc (Southern Biotech #9200-08) at 4 $\mu\text{g}/\text{mL}$, mouse biotinylated-anti-human IgA1 Fc (Southern Biotech #9130-08) at 4 $\mu\text{g}/\text{mL}$, mouse biotinylated-anti-human IgA2 Fc (Southern Biotech #9140-08) at 4 $\mu\text{g}/\text{mL}$ or goat biotinylated-anti-human IgM (Southern Biotech #2020-08) at 3 $\mu\text{g}/\text{mL}$. The samples were tested at a dilution of 1:200 and data are shown as mean MFI + standard deviation (SD) of duplicate measurements from at least two independent experiments. The pre-pandemic controls are shown as mean MFI + SD of 12 samples (Pre, black bar). The horizontal red dotted line represents the cut-off value determined as the mean + 3 SD of 12 pre-pandemic samples for each of the isotypes. (c) Percentages of responders above the cut-off for each spike- or RBD-specific Ig isotype.

a**b****c**

	Linear regression spike MFI		Linear regression RBD MFI	
	r^2	p	r^2	p
Total versus IgG3	0.35	0.0008	0.07	0.15
Total versus IgG4	0.07	0.15	0.24	0.007
Total versus IgA1	0.06	0.20	0.23	0.009
Total versus IgA2	0.06	0.20	0.13	0.05

Fig. 3. IgG1 is the dominant isotype response induced in COVID-19 convalescent individuals. Simple linear regression of (a) spike-specific or (b) RBD-specific total Ig levels versus IgM, IgG1 or IgG2 levels versus (c) spike-specific and RBD-specific IgG3, IgG4, IgA1, and IgA2 levels from the 29 COVID-19-convalescent individuals from Fig. 1. The dash lines represent 95% confidence intervals.

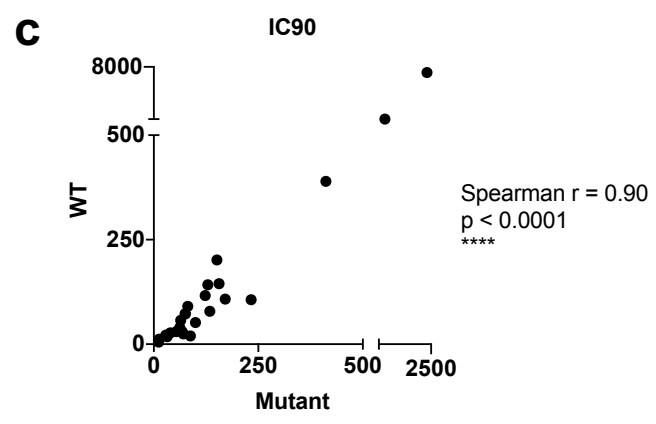
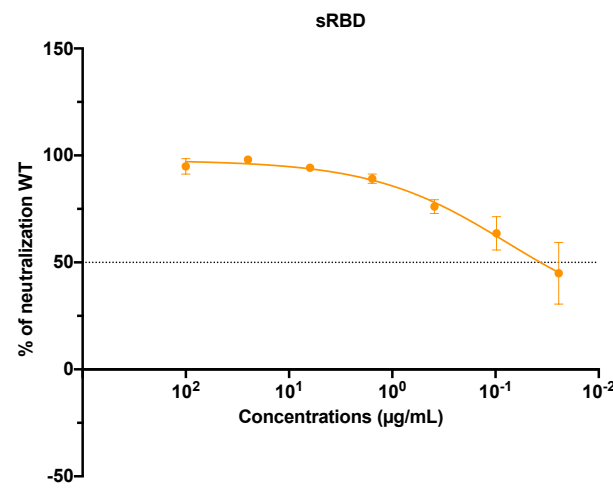
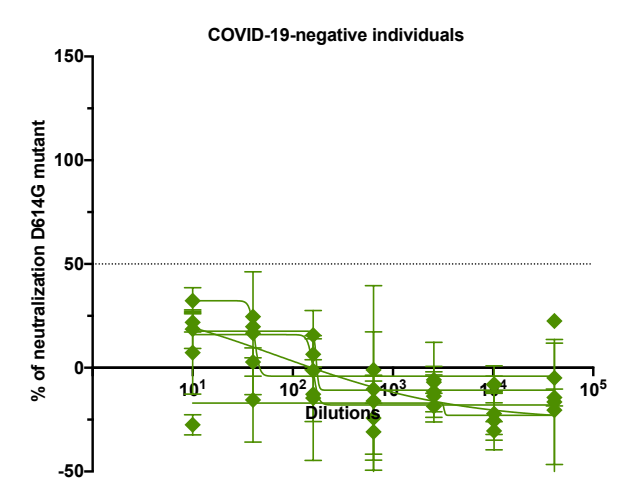
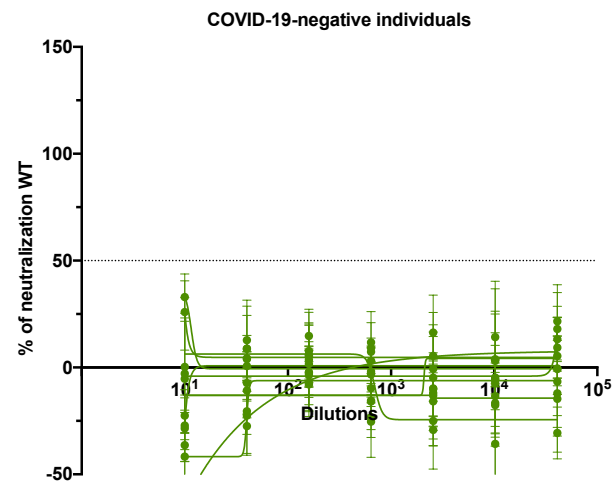
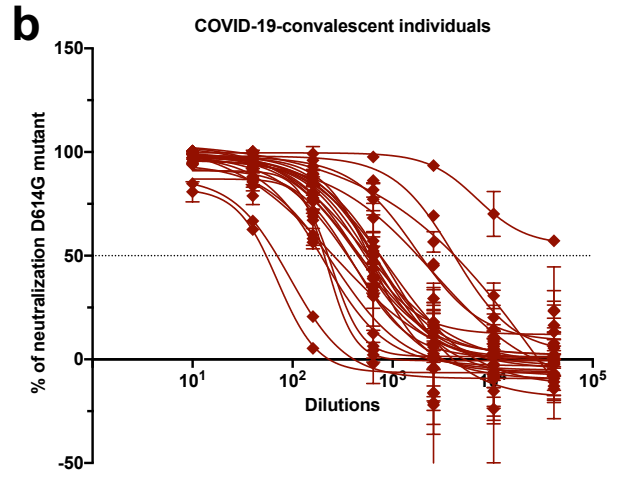
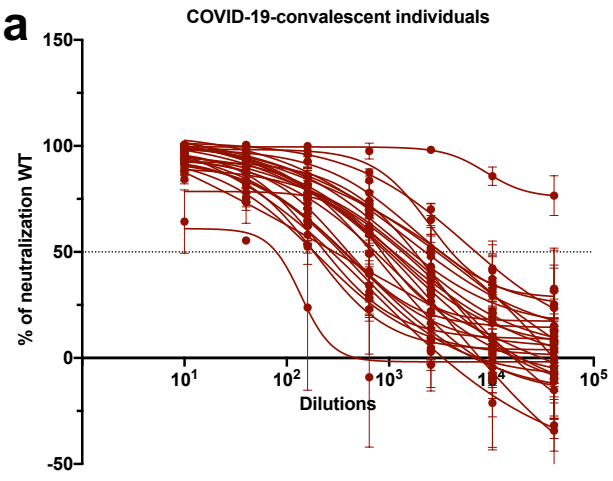


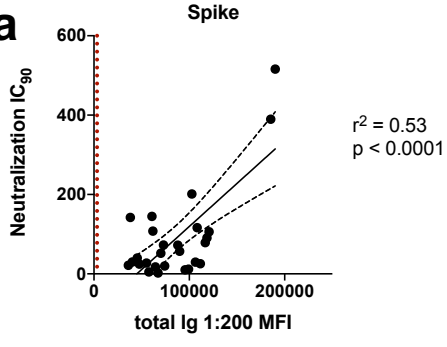
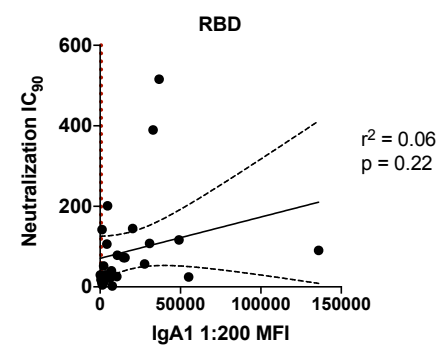
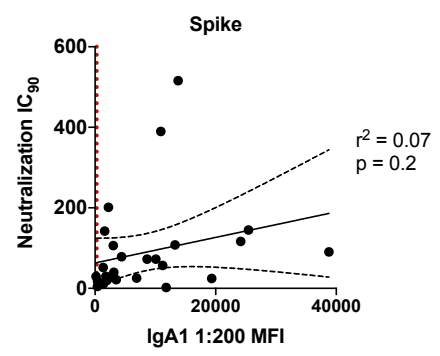
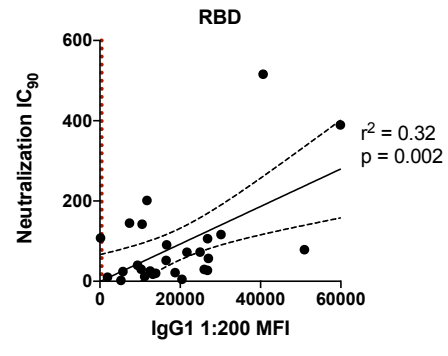
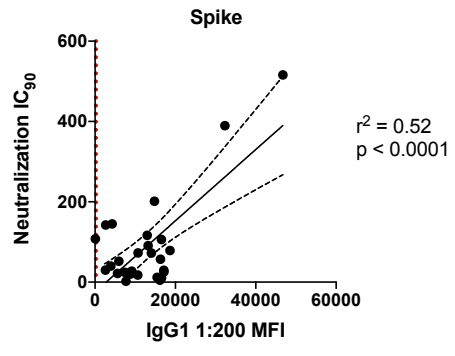
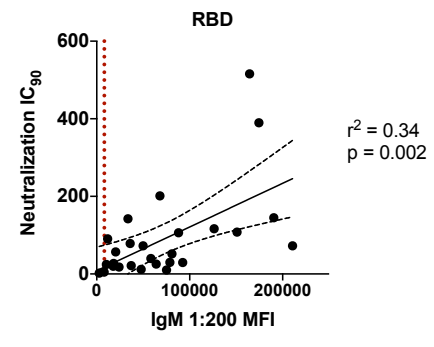
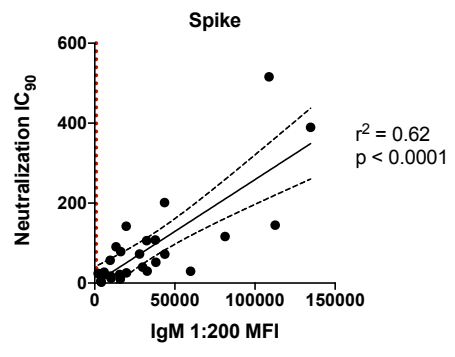
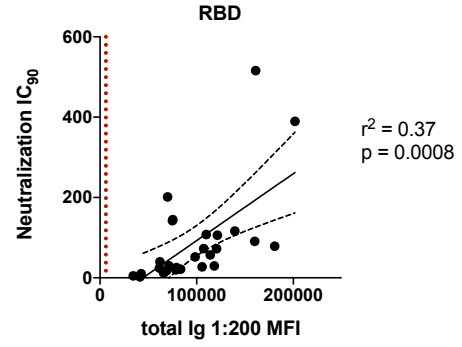
Fig. 4. Neutralization activities are detected in all COVID-19 convalescent individuals.

Neutralization of COV2pp with (a) WT or (b) D614G mutated spike proteins by samples from 28 COVID-19 convalescent individuals and 11 COVID-19 uninfected individuals. The neutralizing activity of recombinant soluble RBD (sRBD) is shown as a positive control.

Twenty-four hours before infection, 20,000 Vero-CCL81 cells/well were seeded. Virus (82.5 μ L/well) was pre-incubated with serially diluted samples (27.5 μ L/well, 4-fold from 1:10 to 1:40,960) for 30 minutes at room temperature. The virus/sample mix was then added to the cells and spinoculated by centrifugation (1250 rpm, 1 hour, room temperature). Six virus-only and six medium-only wells were kept for each plate. After 18 to 22 hours at 37°C, infection was measured by luciferase activity. sRBD was tested as a positive control at 4-fold dilutions from 100 to 0.02 μ g/mL. The data are shown as mean percentage of neutralization + SD of triplicates. The extrapolated titration curves were generated using a nonlinear regression model in GraphPad Prism (Inhibitor versus response – variable slope [four parameters], least squares regression). The dotted horizontal lines highlight 50% neutralization. (c) Spearman correlation between the IC₉₀ titers against COV2pp WT vs. D614G.

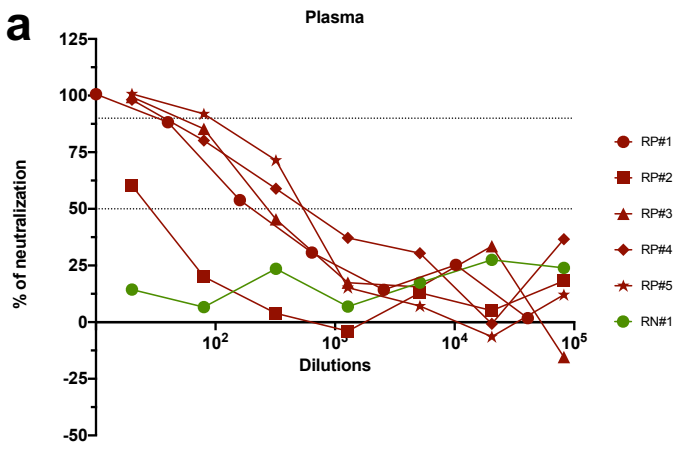
	Sex	Spike								RBD								Neutralization		Neutralization D614G mutant	
		Total Ig	IgM	IgG1	IgG2	IgG3	IgG4	IgA1	IgA2	Total Ig	IgM	IgG1	IgG2	IgG3	IgG4	IgA1	IgA2	IC ₅₀	IC ₉₀	IC ₅₀	IC ₉₀
P#5	unknown	++	+	+	-	-	-	++	-	+	-	+	-	-	-	+	+	36.6	2.3	nd	nd
P#6	unknown	+++	+	++	-	-	+	+	-	++	+	+	-	+	-	+	+	561	26	nd	nd
P#7	unknown	+	++	+	-	-	-	+	-	++	++	+	-	-	-	+	-	nd	nd	nd	nd
P#8	unknown	++	+	++	-	-	+	+	-	+	++	+	-	-	-	+	-	376	10	nd	nd
TF#1	F	+	+	+	-	-	-	+	-	++	+	++	-	-	-	+	-	419	22	255	29
TF#2	M	++	+	++	-	-	-	+	-	++	+	+	-	-	-	+	-	178	12	60	13
TF#3	M	++	+	+	-	-	-	+	-	++	+	+	-	-	-	+	+	165	20	206	88
TF#4	F	+	+	+	-	-	-	+	-	++	+	+	-	-	-	+	-	999	40	329	62
TF#5	M	++++	++	++++	-	-	-	++	-	++++	+++	+++	-	-	-	++	+	2345	516	4138	730
TF#6	F	++	+	+	-	-	-	+	-	++	+	++	-	+	-	+	-	977	52	552	100
TF#7	F	+++	+	++	-	+	-	++++	+	++++	+	++	-	-	-	++++	+	5789	91	453	81
TF#8	M	+	+	+	-	-	-	+	-	++	+	+	-	-	-	+	-	2840	142	700	129
TF#9	F	+++	++	++	-	-	-	+++	+	+++	++	++	-	+	-	++	+	4044	117	664	123
TF#10	M	++	+	+	-	-	-	+	-	+++	+	++	-	-	-	+	+	1060	73	572	75
TF#11	M	++	++++	+	-	-	-	+	-	++	++++	+	-	-	-	+	-	> 40960	7200	> 40960	2344
TF#12	F	+	+	+	-	-	-	+	-	++	++	+	-	-	-	+	-	286	30	326	54
TF#13	M	++	++	+	-	-	-	+++	+	++	+++	+	-	-	-	+	+	1698	145	1573	156
TF#14	M	+++	+	++	-	-	-	+	-	++	+	+	-	+	-	+	-	17079	201	675	151
TF#15	M	+++	+	++	-	-	-	-	-	+++	++	++	-	-	-	-	-	2006	30	549	68
TF#16	M	+++	+	++	-	-	-	+	+	+++	++	++	-	-	-	+	+	1331	106	1961	233
TF#17	M	++	+	+	-	-	-	+	-	+++	+	++	-	-	-	+	-	198	27	186	40
TF#18	F	++	+	++	-	-	-	++	-	+++	+	++	-	-	-	+	+	1122	57	454	64
TF#19	M	++	+	+	-	-	-	+	-	++	+	+	-	-	-	-	-	326	18	201	32
TF#20	F	++	+	++	-	-	-	++	-	+++	+++	++	-	+	-	+	+	1535	72	471	76
TF#21	M	++++	++	+++	-	+	-	++	-	++++	+++	++++	-	-	-	+	+	5376	390	3231	412
TF#22	M	++	+	++	-	-	-	+	-	+	-	++	-	-	-	+	+	623	5	47	12
TF#23	unknown	++	+	-	-	-	-	++	-	+++	+++	-	-	-	-	+	-	3882	108	564	171
TF#24	M	+	+	+	-	-	-	++	+	++	+	+	-	-	+	++	+	814	24	215	71
TF#25	F	+++	+	++	-	-	-	+	-	++++	+	++++	-	-	-	+	-	959	79	605	134

Fig. 5. Summary of relative Ig isotype levels and neutralization titers. Table showing sex (purple, F: female, M: male), relative levels of spike-specific (green) and RBD-specific (blue) Ig isotypes (+: bottom quartile, ++: second quartile, +++: third quartile, ++++: top quartile, -: non-responder) and reciprocal IC50 and IC90 neutralization titers against WT pseudovirus (orange) and D614G pseudovirus (red) of 29 plasma samples from COVID-19 convalescent individuals. nd: not done.

a**b****c**

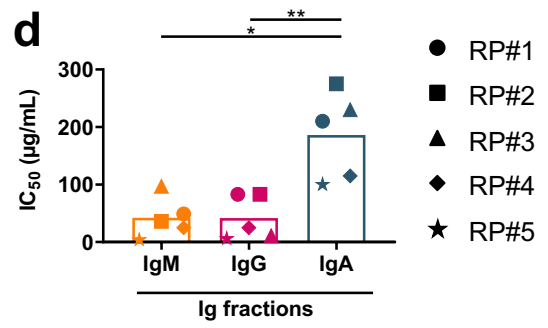
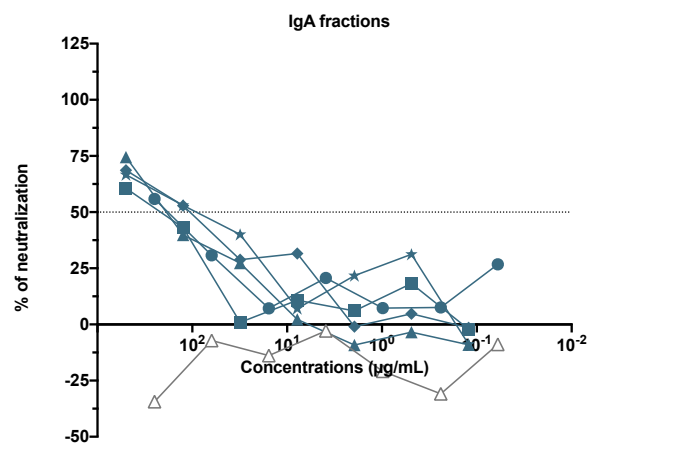
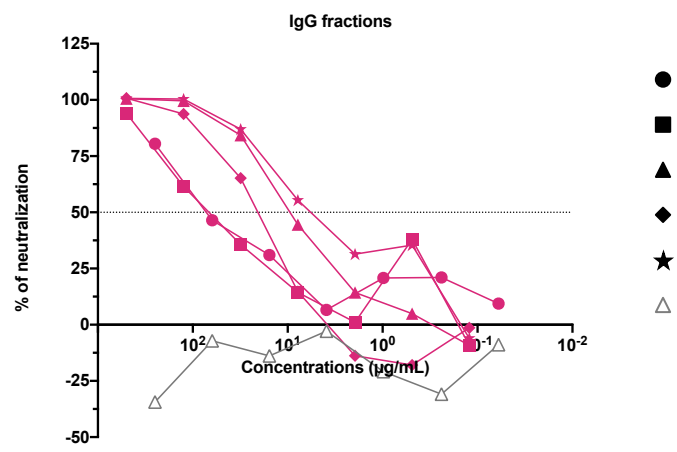
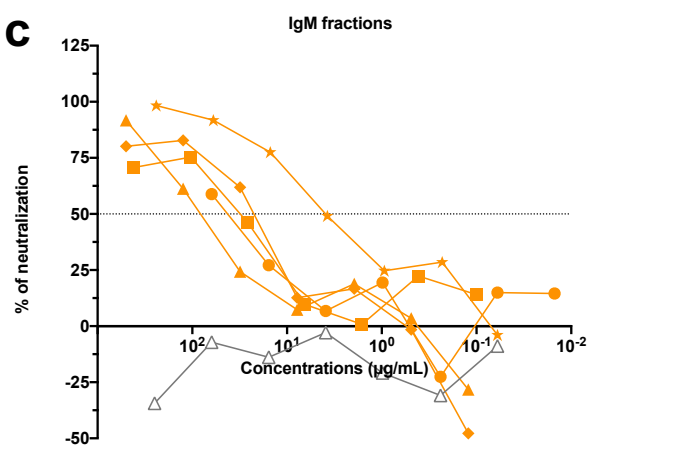
	Linear regression IC ₉₀ versus spike MFI		Linear regression IC ₉₀ versus RBD MFI	
	r ²	p	r ²	p
IgG2	0.14	0.05	0.33	0.002
IgG3	0.30	0.003	0.02	0.46
IgG4	0.00	0.99	0.06	0.21
IgA2	0.02	0.50	0.03	0.45

Fig. 6. IgM and IgG1 contribute most to SARS-CoV-2 neutralization. Simple linear regression of reciprocal IC90 neutralization titers of 27 COVID-19 convalescent individuals versus (a) spike-specific or (b) RBD-specific total Ig, IgM, IgG1 and IgA1 Ab levels. The black dash lines show the 95% confidence intervals. The dotted vertical red line represents the cut-off (mean of 12 pre-pandemic samples + 3 SD) for each isotype from Fig. 1. (c) Statistical results of simple linear regression analyses of reciprocal IC90 neutralization titers of 27 COVID-19 convalescent individuals versus spike-specific or RBD-specific Abs levels for IgG2-4 and IgA2.



b

	Neutralization	
	IC ₅₀	IC ₉₀
RP#1	240	35
RP#2	35	< 20
RP#3	290	60
RP#4	690	45
RP#5	690	100



- RP#1
- RP#2
- ▲ RP#3
- ◆ RP#4
- ★ RP#5
- △ Control Ig

Fig. 7. Purified IgM, IgG, and IgA fractions display neutralizing activities against

SARS-CoV-2. (a) Neutralization of COV2pp by five COVID-19-infected individual plasma samples (RP#1-5) compared to a specimen from a COVID-19 uninfected individual (RN#1, green filled circles). Plasma samples were tested at 4-fold dilutions from 1:10 to 1:40,960 or 1:20 to 1:81,920. Data are shown as the mean percentage of neutralization. The dotted horizontal lines highlight 50% and 90% neutralization. (b) Reciprocal IC50 and IC90 neutralization titers of RP#1-5 plasma samples (c) Neutralization of COV2pp by purified IgM, IgG, and IgA fractions from five COVID-19-infected individuals (RP#1-5) compared to a control Ig fraction (gray open triangles). IgA was isolated first from plasma samples by mixing 1:2 diluted plasma with peptide M agarose beads (600 μ L/28 mL plasma, InvivoGen #GEL-PDM) for 1.5 hours at room temperature. After washing beads, IgA was eluted with a pH 2.8 buffer (Thermo Scientific #21004) and neutralized with pH 9 Tris buffer. The pass-through plasma sample was collected for IgG enrichment using protein G agarose beads (InvivoGen #GEL-AGG) and subsequently for IgM isolation using a HiTrap IgM column (G.E. Healthcare #17-5110-01). An additional purification step was performed using Protein A Plus mini-spin columns to separate IgG from IgM. The fractions were tested at 4-fold dilutions from 500 to 0.02 μ g/mL. Data are shown as the mean percentage of neutralization. The dotted horizontal lines highlight 50% neutralization. (d) IC50 of purified IgM, IgG, and IgA fractions from RP#1-5. The statistical significance was determined by a two-tailed Mann-Whitney test (*: $p < 0.05$, **: $p < 0.01$).